# Diffusion of H in Pd–Ag Alloys (423 to 523 K)

Da Wang*, Ted B. Flanagan*, Kirk Shanahan**,

*Chemistry Department, University of Vermont

Burlington VT 05405,

**Savannah River National Laboratory,

Building 999-2W, Aiken S.C. 29808

**Abstract**

H diffusion constants have been determined from steady-state fluxes through Pd–Ag alloy membranes. The upstream side is maintained at a nearly constant $p_{up}$ and, consequently at nearly constant $r_{up}=H/(Pd_{1-x}Ag_x)$, and the downstream side at $p_{H_2} \approx 0$ ($r_{down}=0$) (423 to 523 K). It is shown that the permeability is a maximum for atom fraction $X_{Ag}=0.23$ at 423, 473 and 523 K at both $p_{up}=20.3$ and 50.5 kPa.

At finite H concentrations non-ideality can be a factor and if concentration-independent diffusion constants, $D_H^*$, are desired the following equation for the flux is appropriate, $D_H^*\left(c_H / RT\right)(dm_H / dx)$, rather than $D_H(c_H)\left(dc_H/dx\right)$. $D_H^*$ can be obtained from obtained from $D_H(c_H)$ using the thermodynamic factor, $\left(\partial \ln p^{1/2}/\partial \ln c_H\right)_T$, which is a function of $r$, and which can be obtained from equilibrium $p_{H_2}$-$r$ isotherms.

The correction for non-ideality is more complex when there is a large H gradient within the membrane as in the present case where $c_{up} \gg c_{down}=0$ because the concentration

and the thermodynamic factor vary with distance through the membrane. This is a very commonly employed situation,

The effect of non-ideality on $D_H$ and $E_D$ has been systematically examined as a function of $X_{Ag}$ for the first time. $D_H$ has been determined for some Pd–Ag alloys as a function of $r$ in the dilute region where $c_{up} \gg c_{down}(=0)$ and, even at small $r$, $D_H$ decreases with $r$ for alloys with $X_{Ag} <$ 0.35. The concentration dependence of $D_H(c_H)$ has been determined for the $Pd_{0.77}Ag_{0.23}$ alloy over a large concentration range.

The activation energies for diffusion, $E_D(r)$ , have been determined as a function of H content in the dilute range and the conversion to concentration-independent $E_D^*$ values has been carried out in several different ways.

The decrease of $D_H$ with $r$ decreases with increase of $X_{Ag}$ and changes sign at $\approx 0.35$. The increase of $E_D$ with $r$ becomes smaller with $X_{Ag}$.

## Introduction

Pd–Ag alloys are the most important Pd alloys with regard to $H_2$ diffusion because the $Pd_{0.77}Ag_{0.23}$ alloy is employed industrially as a $H_2$ purification membrane. There have been many studies of H diffusion in *Pd*–Ag alloys but not much attention has been paid to the role of non-ideality at moderately high temperatures. The dependence of $D_H$ and $E_D$ on the H concentration will be examined here.

H is assumed to occupy octahedral interstices in fcc Pd-rich alloys as it does in pure Pd. Indirect evidence for this is that the inelastic vibrational frequency of H in *Pd*-Ag alloys is characteristic of H in octahedral sites rather than tetrahedral sites [1]. Lovvik and Olson [2] have shown from density functional calculations that H prefers the octahedral sites in *Pd*–Ag alloys.

Solubility and diffusion data from 533 to 913 K are available from Holleck's important work for a series of Pd-Ag alloys [3]. Küssner [4] has determined diffusion data for the $Pd_{0.77}Ag_{0.23}$ alloy using an electrochemical breakthrough

method and he determined $D_H$ as a continuous function of $r$ at 303 K up to H/(Pd$_{0.77}$Ag$_{0.23}$) $=r$, atom ratio,$=0.42$. Bohmholdt and Wicke [5] investigated several Pd-Ag alloys up to $X_{Ag}=0.40$ from 293 to 373 K using a gas phase permeation technique where $X_{Ag}$ is atom fraction Ag and $c_H$ and $r$ are related by $c_H=r\rho/M$ where $\rho$ and M are the density and molar mass of the alloy. They determined $D_H$ values at high and very low $r$. There are several publications by Züchner, et al giving diffusion constants for a series of different Ag composition alloys (296 K) [6]. These workers find that $D_H^*$ values are almost independent of Ag content to about $X_{Ag}=0.30$ (296 K) and then fall abruptly where $D_H^*$ is the concentration-independent diffusion constant.

Thermodynamic parameters and H$_2$ solubilities have been determined elsewhere [7] for the temperature investigated here over a range of H contents in order to obtain diffusion constants from the permeation data to be obtained. A greater number of alloy compositions will be examined in this research than in previous work on these alloys [3, 4, 5, 6].

In H permeation through Pd-based membranes two types of non-ideality should be considered. The first arises from deviations from Sieverts' law of ideal solubility, i.e., when $r \neq K_s p_{H_2}^{1/2}$, and this is easily accounted for if $p^{1/2}$ *vs* $r$ equilibrium isotherms are available. The other type of non-ideality is due to the concentration dependence of Fick's diffusion constant [8], $D_H(r)$. Wicke and co-workers have derived $D_H^*$ from $D_H(r)$ values for Pd and some of its alloys [8] using equation (1). When it is desired to determine the role of f($r$), the thermodynamic factor, on $D_H$, electrochemical time-lag techniques are frequently employed where a membrane, initially charged homogeneously with H, is electrochemically perturbed on the upstream side and the break-through time needed for the perturbation to reach the downstream side can be used to calculate $D_H(c_H)$ [4, 6, 8]. In these experiments where the $r$ does not change very much an average value can be employed in equation (1).

$$D_H(r)=D_H^* \left( \frac{\partial \ln p_{H_2}^{1/2}}{\partial \ln r} \right)_T = f(r)D_H^* \tag{1}$$

Salomons, et al [9, 10] measured the dependence of $D_H$ on $r$ for Pd, a $Pd_{0.80}Cu_{0.20}$ alloy and a disordered $Pd_{0.91}Y_{0.09}$ alloy at elevated temperatures using a gravimetric method to determine the relaxation times, and thus $D_H$ values, for H uptake following sudden $p_{H_2}$ changes. Details of the extent of the $p_{H_2}$ change and the accompanying change of $c_H$ were not provided. They found a decrease in $D_H$ with $r$ which they explained using the thermodynamic factor and a site blocking (1–r) factor.

Subsequently, Stonadge, et al [11] employed the same technique as Salomons [9] for an ordered $Pd_{0.90}Y_{0.10}$ alloy, however, there was no comparison of the results of the two investigations. Stonadge, et al determined concentration-independent diffusion constants, $D_H^*$, for the ordered form of this alloy using isotherms to evaluate the thermodynamic factor. From 463 to 540 K the $D_H^*$ were not constant but increased with $c_H$ which they attributed to unspecified traps.

In experiments where $D_H$ is determined from steady state fluxes there is, most commonly, a large concentration profile within the membrane, e.g., $p_{up}$ is large and $p_{down}$ small and it may be inappropriate to employ equation (1) directly; the subscripts up and down refer to the high and low pressure sides of the membrane. Recently a procedure has been given for determining Einstein's diffusion constants from the concentration-dependent ones for this steady state situation [12].

It has been shown recently for Pd membranes [13] that even when $c_{up} \gg c_{down} = 0$, an average concentration can be employed in equation (1) provided that $r$ is small, i.e., $f(r_{av}) \approx f(r_{up})/2$. This gives reasonable agreement with more exact methods at small $r$. This approximation may, however, not be appropriate for all the Pd–Ag alloy membranes as will be shown below.

## Experimental

The alloys and membranes were prepared by arc-melting the pure components and then annealing at 1123 K for 72 h and then rolling and re-annealing.

The flux was determined from the decrease of $p_{H_2}$ on the upstream side of the membrane using an MKS gauge and the downstream side was kept at $p_{H_2} \approx 0$ [14]. The steady state fluxes were established very quickly for these Pd–Ag alloy

membranes at the temperatures employed. There was a small fall-off in flux during the measurements due to the decrease in $p_{up}$ but this was generally small because the upstream volume is large and, in any case, the flux can be corrected for such small decreases. Generally, however, the fluxes were taken as initial ones before any appreciable decrease of $p_{up}$. The areas of the membranes were all the same, 1.77 cm$^2$. The membrane was enclosed by a tube furnace controlled to about $\pm 1\,^\circ$C. The temperatures were set by an electronic controller and they were found to be in good agreement with those measured by a temperature sensor in direct contact with the mounted membrane.

The membranes were oxidized in the atmosphere for $\approx$30 min at 953 K before mounting them in the diffusion apparatus since this procedure has been shown to improve the reproducibility of the membranes [14]. Since oxides formed by Pd or Ag do not penetrate into the alloy appreciably and are rapidly reduced in the presence of $H_2$, the membrane thicknesses are taken as those before oxidation.

## Results and Discussion

The flux of H in the present experiments, where the downstream side is maintained at $p_{H_2} \approx 0$, is given by

$$J \; ((mol\;H/s)/cm^2) = -\,D_H\,(\,dc_H\,/\,dx) \approx -\,D_H\,c_{up}\,/\,d \quad (2)$$

where J is the flux and d the membrane thickness. The diffusion constants were determined from the fluxes using isotherms given elsewhere [7].

The first part of the paper will deal with demonstrations that under the conditions employed, bulk diffusion is the slow step in these membranes. The second part will concern trends of the concentration-dependent $D_H$ and $E_D$ with *r*. These diffusion parameters are technologically important because they determine the actual permeabilities under the conditions of $p_{H_2}$ and temperature employed. The third part will deal with quantitative understanding of the concentration dependence of $D_H$ and $E_D$ and the determination of the fundamental, concentration-independent parameters, $D_H^*$ and $E_D^*$.

**Evidence for Bulk Diffusion Control in Pd–Ag Alloys**

Under experimental conditions similar to those employed here, it was shown earlier [13, 14] that bulk diffusion is the rate controlling step for pure Pd membranes. Since the H permeability is greater for some of the *Pd*–Ag alloys, e.g., $Pd_{0.77}Ag_{0.23}$, than for Pd, it must be shown that bulk diffusion is also the

controlling step for the Pd–Ag alloys. The $Pd_{0.77}Ag_{0.23}$ alloy was chosen for this purpose because it has the greatest H permeability and because it is the alloy composition generally employed for $H_2$ purification.

Figure 1 shows a plot of the specific permeabilities, $P = D_H K_s' p_{H_2}^{1/2}$, of $Pd_{0.77}Ag_{0.23}$ alloy membranes as a function of $p_{H_2}^{1/2}$ at 473 K where $K_s'$ relates $c_H$ with $p_{H_2}^{1/2}$, i.e., Sieverts law of ideal solubility for a dissociating gas, $c_H = K_s' \times p_{H_2}^{1/2}$. Figure 1 shows that the relation is linear only at small $r$ and at higher concentrations there are deviations due to the dissolved H no longer obeying Sieverts' law of ideal solubility. The initial linear slope indicates that bulk diffusion is the controlling step for permeation but it would be more convincing if these data obeyed the $P$ $v.s.$ $p_{H_2}^{1/2}$ relation over the entire range. The basic problem is that Sieverts' law of ideal solubility does not hold over this whole $p_{H_2}$ range and therefore this must be allowed for. The $p_{H_2}$-$r$ isotherm at this temperature for this alloy [7] can be employed to allow for this non-ideality. The experimental $p_{exp.}^{1/2}$ values have been multiplied by the ratios $\left( p_{ideal} / p_{exp.} \right)^{1/2}$ to give an ideal $p_{ideal}^{1/2}$ at each permeability. When this is done, a corrected relationship is obtained which is quite linear (Fig. 1) indicating that bulk diffusion is the slow step over the entire range.

Another, and better, test for bulk diffusion as the controlling step is a linear dependence of flux, J, on 1/d where d is the membrane thickness. Such experiments have been carried out here with the $Pd_{0.77}Ag_{0.23}$ alloy where Figure 2 shows J $versus$ 1/d at $p_{up} = 50.6$ kPa and 473 K over a range of membrane thicknesses from d=120 to 305 μm. At constant $p_{H_2}$ and temperature, non-ideality due to the thermodynamic factor, equation (1), does not depend on d and thus will not influence the linearity. The observed linearity in Figure 2 shows that bulk diffusion is the controlling step. J should approach zero as (1/d) $\rightarrow$0 and it is seen that the data extrapolate linearly to the origin.

From the results in Figures 1 and 2 it can be concluded that bulk diffusion is the controlling step for H permeation through the $Pd_{0.77}Ag_{0.23}$ alloy and since its

permeability is the greatest of the Pd–Ag alloys, it seems safe to conclude that bulk diffusion is also the rate controlling step for the other alloys.

# Dependence of Permeabilities and Diffusion Parameters, $D_H$, $E_D$ and $\overset{\circ}{D}_H$, on $X_{Ag}$.

## H Permeabilities as a Function of $X_{Ag}$ in *Pd-Ag* Alloys

The permeabilities at 423, 473, 523 K for $p_{up}$=20.3 kPa and 50.6 kPa are shown in Figures 3 and 4, respectively, where the permeability in these Figures is defined as $P$=J×d, i.e., where $K'_S p^{1/2}$ has been replaced by $c_H$ using the isotherms [7]. The permeability is greatest for the $Pd_{0.77}Ag_{0.23}$ alloy which, together with the fact that it does not form a hydride phase at T≥298 K, are the reasons it is employed as a $H_2$ purification membrane.

The permeability is proportional to $D_H \times c_H$ and the $D_H$ values are similar for the Pd–Ag alloys up to about $X_{Ag}$≈0.30 [3, 6] and then they decline as will be shown below. At 20.3 kPa (Fig. 3) the $H_2$ solubilities are greater in the $X_{Ag}$=0.23 alloy than in those with $X_{Ag}$<0.23 at all three temperatures [7] and, although for some alloys with $X_{Ag}$>0.23 the $H_2$ solubilities are greater, their $D_H$ values are smaller and therefore the permeabilities will be smaller. For the higher $p_{H_2}$=50.6 kPa (Fig. 4) the solubilities are greater at 473 and 523 K for $X_{Ag}$=0.23 alloy than for those with $X_{Ag}$<0.23, however, this is not the case at 423 K where the solubilities are greater for the $X_{Ag}$<0.23 alloys even though the permeability is greater for $X_{Ag}$ =0.23 (Fig. 4). It should be realized at these relatively large H contents non-ideality due to the thermodynamic factor, f(r), will be appreciable. Evidence will be presented that the greater permeability of the $X_{Ag}$=0.23 alloy at 423 K is due to this non-ideality which causes $D_H$ to be greater for this alloy at this *r* as compared to those with $X_{Ag}$<0.23.

## Fick's Diffusion Constants at Constant $p_{H_2}$ and at Constant $c_H$.

Fick's concentration-dependent diffusion constants, $D_H(r)$ , can be readily determined using equation (2) from the flux, $p_{up}$, and the isotherms needed to obtain $r_{up}$ (or $c_{up}$) from $p_{up}$. These concentration-dependent $D_H(r)$ are important

for the practical use of Pd–Ag membranes because the flux is determined by $D_H \times c_H$ for a given membrane geometry and temperature (eqn. (2)). $D_H(r)$ values have been determined here for the Pd–Ag alloys both at constant $r_{up}$ and at constant $p_{up}$ over the temperature range from 423 to 523 K which is relevant for $H_2$ purification applications. Table 1 shows $D_H$ values all determined at $p_{up}$=20.3 kPa.

Table 1:  $D_H/10^{-6} cm^2/s$ measured with $p_{up}$=20.3 kPa for Pd-Ag Alloys (423-523 K)*

| $X_{Ag}$ | $D_H /10^{-6} cm^2 / s$ | | | | |
|---|---|---|---|---|---|
| | 423 K | 453 K | 473 K | 503 K | 523 K |
| 0 | 5.3 | - | 12.4 | - | 21.8 |
| 0.10 | 4.5(4.4) | 7.8(7.2) | 10.7(9.8) | 15.0(14.2) | 18.9(17.9) |
| 0.15 | 3.4(3.5) | 6.4(6.4) | 8.7(8.8) | 13.3(13.2) | 15.9(16.0) |
| 0.19 | 2.7(2.3) | 5.5(5.6) | 8.0(7.8) | 12.3(11.9) | 14.7(14.6) |
| 0.23 | 2.6(2.6) | 4.9(4.9) | 6.6(6.7) | 9.8(9.8) | 12.5(12.6) |
| 0.30 | 2.5(2.3) | 4.0(3.9) | 5.3(5.2) | 8.1(7.8) | 9.9(9.7) |
| 0.35 | 2.0 | 3.0 | 3.9 | 5.9 | 7.5 |
| 0.40 | 1.4 | 2.2 | 2.7 | 4.0 | 5.0 |
| 0.45 | 0.77 | 1.2 | 1.6 | 2.4 | 3.0 |
| 0.50 | 0.33 | 0.60 | 0.84 | 1.2 | 1.6 |

 * the values with and without parenthesis represent different sets of alloy membranes and measurements.

Measurements were repeated with two sets of alloys from different preparations. The results in parenthesis (Table 1) are the most recent. The results are similar and differences between the two can be attributed to experimental error in J measurements, to compositional variations of the alloys and to the measurement of d. It can be seen from the Table that $D_H(r)$ values do not vary much with $X_{Ag}$ until >0.30 where there is a marked fall-off.

Figure 5 shows $\log D_H(r)$ as a function of $X_{Ag}$ at $p_{up}$=20.3 kPa and 473 K. There is a small decrease with $X_{Ag}$ to about 0.30 and then a stronger decrease. The $D_H$ values agree reasonably well at low $X_{Ag}$ but are larger at higher $X_{Ag}$ than those predicted using the equation given by Holleck [3] based on his data from a higher temperature range. The influence of the non-ideality from the thermodynamic factor increases with decrease of temperature and varies with $X_{Ag}$ which will be discussed below.

$D_H(r)$ values were also determined over this same temperature range for these alloys at constant $r_{up}$ values, e.g., $r_{up}$=0.03, 0.04, etc. The same trend with $X_{Ag}$ is found for these constant H concentration values but their magnitudes differ somewhat from those at constant $p_{H_2}$ due to the role of thermodynamic factor which depends on $r$ and temperature. These results will be discussed below.

## Activation Energies for Fick's Diffusion Constants

Activation energies for diffusion, $E_D$, were determined from the temperature-dependence of the fluxes at constant $c_{up}$. From equation (2), $\ln J=-[\ln D_H+ \ln c_{up}-\ln d]$ and the derivative of this equation with respect to 1/T at constant $c_{up}$,($\propto r_{up}$), gives activation energies. It follows from this equation that $E_J=E_D$ where $E_J$ is the activation energy for the flux determined at constant $c_{up}$. Plots of quantities proportional to the fluxes, normalized to 100 μm, are plotted as ln against 1/T in Figure 6 where $r_{up}$ has been held constant for each alloy. The H contents held constant, $r_{up}$, are not the same for each alloy varying between $r$=0.03 ($X_{Ag}$=0.10) and 0.08 ($X_{Ag}$=0.50) (Fig. 6). The equilibrium pressures decrease with $X_{Ag}$ making it difficult to measure them at low $r_{up}$ for the higher Ag content alloys and therefore $r_{up}$ had to be greater for the larger $X_{Ag}$ alloys. It can be seen that as $X_{Ag}$ increases, the slopes of the plots and their intercepts become more negative. Table 2 shows values of $E_D$ determined at these constant H contents and also gives pre-exponential factors, $\overset{\circ}{D_H}$. Parameters for Pd are also shown.

Activation energies for permeability, $E_P$, have been derived from the relation $E_P=E_D+\Delta \overset{\circ}{H_H}$ where $E_D$ is positive and $\Delta \overset{\circ}{H_H}$ is negative and the standard state

designation on the enthalpy of $H_2$ solution refers to infinite dilution of H. This equation follows from equation (2) and $P=J\times d$. The $\Delta H_H^o$ are available for these alloys elsewhere [16].

Figure 7 shows $E_D$ plotted along with $E_P$ as a function of $X_{Ag}$ where $E_D$ has been determined from the constant $r$ plots (Fig. 6). The trend in $E_D$ agrees with that found by Holleck [3] and Opara, et al [6] in that the $E_D$ are reasonably constant and nearly equal to that for Pd up to about $X_{Ag} \approx 0.30$ and then $E_D$ increases. The location of the minimum in $E_P$ shown in Figure 7 does not agree exactly with Figures 3 and 4 because the pre-exponential factors also affect the permeabilities.

Table 2:   $E_D$ for Pd-Ag Alloys (423-523 K) Determined at Constant Small $r_{up}$ Values as shown in the Table.

| $X_{Ag}$ | $r_{up}$ | $E_D(1)$  /kJ/ mol H | $E_D(2)$   /kJ/ mol H | $D_H^o$  /(cm$^2$/s)/10$^{-3}$ |
|---|---|---|---|---|
| 0 | - | 23.5 | 23.5 | 4.8 |
| 0.10 | 0.03 | 23.8 | 23.3 | 3.6 |
| 0.15 | 0.04 | 23.7 | 23.6 | 3.5 |
| 0.19 | 0.05 | 23.4 | 24.1 | 3.6 |
| 0.23 | 0.05 | 23.2 | 23.7 | 2.8 |
| 0.30 | 0.06 | 24.4 | 25.6 | 3.5 |
| 0.35 | 0.07 | 26.85 | 27.7 | 4.4 |
| 0.40 | 0.075 | 28.9 | 29.1 | 3.8 |
| 0.45 | 0.05 | 30.7 | - | 1.6 |
| 0.50 | 0.08 | 33.1 | 33.8 | 3.8 |

Log $c_H$/mol H/cm$^3$ and log $D_H$/(cm$^2$/s)    are plotted against 1/T in Figure 8 for the $Pd_{0.77}Ag_{0.23}$ alloy. Their sum, which is proportional to log(permeability), is shown after translation along the y-axis in order for it to coincide with the intersection of the $c_H$/mol H/cm$^3$ and log $D_H$/(cm$^2$/s)    lines. It can be seen that the sum is nearly independent of T. This indicates that the permeability of a $Pd_{0.77}Ag_{0.23}$ membrane, which is used industrially for $H_2$ purification, does not increase by going to higher temperatures explaining why there is not much difference in the permeabilities at the different temperatures as shown in Figures 3, 4.

## Concentration Dependence of $D_H$ and $E_D$ Values for the $Pd_{0.90}Ag_{0.10}$, $Pd_{0.77}Ag_{0.23}$, $Pd_{0.65}Ag_{0.35}$ and $Pd_{0.50}Ag_{0.50}$ Alloy Membranes.

These four alloy compositions have been chosen for detailed examination of the dependence of $D_H$ and $E_D$ on $r$ because it was not feasible to examine all of the alloy compositions in detail and these alloy compositons are representative of the various types of behavior. Experimental values of ln $D_H$ (423 K) and $E_D$ (423 to 523 K) are shown for the $Pd_{0.90}Ag_{0.10}$ alloy (423 K) in Figure 9. ln $D_H$ is seen to decrease with $r$ which is the same trend as for Pd–H, however, the slopes are not as steep as those found for Pd [13]. There seems to be two slopes, one at low $r$ and the other at higher $r$. Extrapolation to $r$=0 seems to be satisfactory giving $D_H^*$=5.6×10$^{-6}$cm$^2$/s. The extrapolation of $E_D$ to $r$=0 appears to give a value which is too small, however, this may be within the margin of error.

Figure 10 shows the dependence of ln $D_H$ and $E_D$ on $r$ for the important $Pd_{0.77}Ag_{0.23}$ alloy membrane and detailed results are given in Table 3 for three of the five temperatures measured. It can be that at all three temperatures $D_H$ decreases with $r$.

It is difficult to extrapolate experimental ln $D_H$ to $r_{up}$=0 for this alloy (Fig. 10) because the lowest values of $r$ are too high for meaningful extrapolations except at 473 K where the data appear to extrapolate to 7.4×10$^{-6}$/cm$^2$/s which is in reasonable agreement with the $D_H^*$ determined by other methods (Table 3).

The dependence of $\ln D_H$ and $E_D$ on $r$ for the $Pd_{0.65}Ag_{0.35}$ alloy membrane is shown in Figure 11 and for this alloy they appear to be nearly independent of $r$, in contrast, to the lower Ag content alloys (Figs. 9, 10).

The $Pd_{0.50}Ag_{0.50}$ alloy is of interest because the thermodynamic factor is positive at low $r$ which should cause $D_H$ to increase, rather than decrease, with $r$ as for the lower Ag content alloys. Results are shown in Figure 12 and tabulated in Table 4 where it can be seen that at, e.g, 523 K there is a steady *increase* of $D_H$ with $r$ as expected.

Figure 13 shows plots of $\ln D_H/cm^2/s$ against $r$ for Pd and for the $Pd_{0.90}Ag_{0.10}$, $Pd_{0.77}Ag_{0.23}$, and $Pd_{0.65}Ag_{0.35}$ alloys at 423 K. This temperature has been chosen for this plot because the non-ideality is greater at the lower temperature. It can be seen that $\ln D_H$ decreases with $X_{Ag}$ and the slopes (negative) of the plots also decrease progressively with increase of $X_{Ag}$.

Table 3: $D_H \times 10^6$ in units of $cm^2/s$ as a function of $r_{up}$ for the $Pd_{0.77}Ag_{0.23}$ Alloy

| 423 K | | | | |
|---|---|---|---|---|
| $r_{up}$ | $D_H(exp)$ | $D_H^*$ (RIS) | $D_H^*$ (F($r$)) | $D_H^*$ F($r$) at ($r_{up}$/2) |
| 0.040 | 3.37 | 3.89 | 3.85 | 3.87 |
| 0.050 | 3.25 | 3.89 | 3.87 | 3.89 |
| 0.060 | 3.13 | 3.89 | 3.86 | 3.86 |
| 0.070 | 3.05 | 3.95 | 3.86 | 3.96 |
| 0.080 | 2.95 | 3.99 | 3.82 | 4.10 |
| 473 K | | | | |
| 0.020 | 7.13 | 7.47 | 7.51 | 8.04 |
| 0.030 | 7.02 | 7.53 | 7.62 | 8.25 |
| 0.040 | 6.92 | 7.60 | 7.68 | 8.44 |
| 0.050 | 6.78 | 7.64 | 7.68 | 8.15 |
| 0.060 | 6.64 | 7.68 | 7.67 | 8.03 |
| 0.070 | 6.43 | 7.63 | 7.61 | 7.86 |
| 0.080 | 6.27 | 7.64 | 7.57 | 7.74 |
| 523 K | | | | |
| 0.040 | 12.20 | 13.27 | 13.15 | 13.20 |
| 0.050 | 12.14 | 13.48 | 13.33 | 13.48 |
| 0.060 | 12.04 | 13.67 | 13.49 | 13.68 |
| 0.070 | 11.88 | 13.80 | 13.55 | 13.42 |
| 0.080 | 11.68 | 13.89 | 13.55 | 13.61 |

Table 4:  $D_H \times 10^6$ as a function of $r_{up}$ for the $Pd_{0.50}Ag_{0.50}$ Alloy.

| 423 K | | |
|---|---|---|
| $r_{up}$ | $D_H(exp)/10^{-6}cm^2/s$ | $D_H^*/10^{-6}cm^2/s(F(r))$ |
| 0.040 | 0.29 | 0.22 |
| 0.045 | 0.31 | 0.22 |
| 0.050 | 0.34 | 0.22 |
| 0.055 | 0.37 | 0.25 |
| 0.060 | 0.40 | 0.24 |
| 0.065 | 0.43 | 0.23 |
| 473 K | | |
| 0.030 | 0.72 | 0.68 |
| 0.035 | 0.75 | 0.73 |
| 0.40 | 0.78 | 0.76 |
| 0.045 | 0.82 | 0.77 |
| 0.050 | 0.85 | 0.80 |
| 0.060 | 0.94 | 0.80 |
| 523 K | | |
| 0.025 | 1.54 | 1.39 |
| 0.030 | 1.62 | 1.43 |
| 0.035 | 1.69 | 1.42 |
| 0.040 | 1.75 | 1.43 |
| 0.045 | 1.83 | 1.46 |
| 0.050 | 1.88 | 1.45 |

# Quantitative Description of the Concentration-Dependence of $D_H$ and $E_D$ and the derivation of Concentration-Independent Diffusion Parameters.

In this section the dependence of $D_H$, Fick's diffusion constant, and $E_D$ on $r$ will be considered. For example, the slopes of plots of $\ln D_H$ against $r$ will be evaluated for the various alloys and compared to the predicted ones. The concentration-independent parameters, e.g., $D_H^*$, will be determined from the concentration-dependent ones, e.g., $D_H$. The role of non-ideality due to the thermodynamic factor has been discussed for pure Pd in some detail elsewhere for the present experimental situation where $r_{up} \gg r_{down}$ [13] and will be briefly summarized here for the Pd–Ag alloys. Again, the $Pd_{0.77}Ag_{0.23}$ alloy will be employed for illustration because of its importance.

**Concentration Independent $D_H^*$ from the Experimental $D_H(r)$ Values at Small H Contents**

The slopes of $\ln p_{H_2}^{1/2}$-$\ln r$ isotherms, such as shown in Figure 14 for the $Pd_{0.77}Ag_{0.23}$ alloy, give the thermodynamic factor, $\left( \partial \ln p_{H_2}^{1/2} / \partial \ln r \right)_{T,X_{Ag}} = f(r)$. A plot of f($r$) as a function of $r$ can then be made for each alloy at each temperature. Figure 15 shows such a plot for the $Pd_{0.77}Ag_{0.23}$ alloy at 423 K from which values of $F(r_{up})$ can be obtained by integration according to equation (3). At this temperature and for this alloy, the thermodynamic factor, f($r$), first decreases and then increases with $r$. $D_H^*$ can be calculated at any value of $r_{up}$ with $r_{down} = 0$ using

$$D_H(r) = D_H^* \int_0^{r_{up}} \left( \frac{\partial \ln p_{H_2}^{1/2}}{\partial \ln r} \right) dr / r_{up} = D_H^* F(r_{up}) / r_{up}.$$  (3)

This equation was given in [12] and used for Pd–H in [13] to obtain $D_H^*$ values.

Metal-H systems have been described successfully at low H contents by simple statistical thermodynamic equations which can be employed to evaluate F($r$) in

equation (3). The simplest one is the regular interstitial solution (RIS) [17] or mean field, lattice gas model,

$$RT \, \ln p_{H_2}^{1/2} = \Delta \mu_H^{\circ} + RT \, \ln \left( \frac{r}{1-r} \right) + g_1 \times r \qquad (4)$$

where $g_1$ is the linear term of a polynomial expansion of $\mu_H^E(r)$ in $r$ and is a constant at a given temperature for a given alloy. Experimental isotherms are needed to evaluate $g_1$, it is negative for Pd but becomes less negative with $X_{Ag}$, until at large $X_{Ag}$, it is positive [7]. Values of $g_1$ for the alloys have been evaluated using $\beta=1.0$ in the configurational partial entropy term, $-R\ln(r/(b-r))$, which is not strictly correct because of selective occupation of interstices in Pd–Ag alloys and therefore $\beta \neq 1.0$. Nonetheless, $\beta$ will be taken as 1.0 and this will not affect the use of the thermodynamic factor, f(r), for obtaining, e.g., $D_H^*$.

From this model the following equation is obtained for F(r) [13]

$$F(r_{up}) = -\ln(1 - r_{up}) + g_1 r_{up}^2 / 2RT. \qquad (5)$$

Using this result, equation (6) can be derived

$$D_H = D_H^* \left( \frac{g_1 r_{up}}{2RT} - \frac{\ln(1 - r_{up})}{r_{up}} \right). \qquad (6)$$

Under conditions where $c_{up} \gg c_{down}$, it was found for Pd–H that an average value of $r$ can be employed in equation (1) giving reasonable values of $D_H^*$ from $D_H(r)$ [13]. The assumption that $r_{av} \approx r_{up}/2$ at small $r_{up}$ provides a somewhat simpler procedure than the other procedures for the determination of $D_H^*$. Although this is a good approximation for Pd–H at small $r$, it may not be for some of the Pd–Ag alloy membranes and this will be examined here.

Table 3 shows values of $D_H^*$ for the $Pd_{0.77}Ag_{0.23}$ alloy from $D_H(r)$ at different $r$ values using three different methods, i.e., equation (6), equation (3) with F(r) values determined from plots such as shown in Figure 15 for the $Pd_{0.77}Ag_{0.23}$ alloy and using the approximation $f(r_{up}/2) = f(r_{av})$ in equation (1). It can be seen that generally the $D_H^*$ values are more constant than the $D_H$ values and the former

are generally greater than the latter as expected. It can also be seen that the approximation, $f(r_{up}/2) = f(r_{av})$, gives somewhat greater values at 473 K but is otherwise not a bad approximation for small $r$.

Using the data employed for Figure 6, $D_H^*$ values were obtained for all of the alloys. These are shown in Table 5 at 423, 473 and 523 K where $p_{H_2} = 20.3$ kPa but at 423 K only the $Pd_{0.90}Ag_{0.10}$ and $Pd_{0.81}Ag_{0.19}$ alloys were determined at 20.3 kPa while the remainder were determined at the $r$ indicated. The $D_H^*$ shown in Table 5 for the $Pd_{0.77}Ag_{0.23}$ alloy differ slightly from those in Table 3 because the former were determined with a different membrane and consequently errors enter due to the thickness measurements. The $D_H^*$ in Table 5 show the same trend with $X_{Ag}$ as the $D_H$ values in Figure 5.

From equation (6) at small $r$, the slopes are given by $g_1/2RT$. These values of $g_1$ can be compared with those obtained from thermodynamic data, i.e., plots of $RT \ln p^{1/2}[(1-r)/r)]$ against $r$ [7]. The slopes of the plots in Figure 13 give $g_1$ (Pd)=–49.0 kJ/mol H (–35.9 kJ/ mol H), $g_1$ ($Pd_{0.90}Ag_{0.10}$)=–39.8 kJ/mol H (–34.7 kJ/ mol H), $g_1$ ($Pd_{0.77}Ag_{0.23}$)=–23.5 kJ/mol H (–22.7 kJ/ mol H) and $g_1$ ($Pd_{0.65}Ag_{0.35}$)=–5.4 kJ/mol H (–11.3 kJ/ mol H) where the values in parenthesis are from thermodynamic measurements. The agreement is good for the $Pd_{0.90}Ag_{0.10}$ and $Pd_{0.77}Ag_{0.23}$ alloys demonstrating the validity of the analysis, however, the agreement is not as good for Pd and the $Pd_{0.65}Ag_{0.35}$ alloy.

Table 5: $(D_H^*/cm^2/s) \times 10^{-6}$  obtained from $D_H(r)$ at $p_{up}$=20.3 kPa except for some at 423 K where the *r* values employed are shown in parenthesis*

| % Ag | T/K | $D_H(r)$ | $D_H^*(F(r))$ | $D_H^*(RIS)$ | $D_H^*(extrap)$ |
|------|-----|----------|---------------|--------------|-----------------|
| 10 | 423 | 4.4 | 4.6 | 4.7 | 6.0 |
| 19 | 423 | 3.5 | 6.4 | - | 6.6 |
| 23 | 423 | 3.4(0.04) | 4.0 | 3.9 | 3.9 |
| 30 | 423 | 2.4(0.06) | 2.7 | 2.6 | - |
| 40 | 423 | 1.4(0.06) | 1.3 | 0.88 | - |
| 50 | 423 | 0.27(0.04) | 0.22 | 0.17 | - |
| 10 | 473 | 9.8 | 10.9 | 10.2 | 10.9 |
| 15 | 473 | 8.8 | 9.7 | 9.3 | 10.2 |
| 19 | 473 | 7.8 | 9.7 | 8.0 | 9.6 |
| 23 | 473 | 6.7 | 8.1 | 7.6 | 8.3 |
| 30 | 473 | 5.2 | 5.8 | 5.2 | 6.7 |
| 35 | 473 | 4.2 | 4.2 | - | 4.7 |
| 40 | 473 | 2.7 | 2.6 | - | 2.8 |
| 45 | 473 | 1.6 | 1.4 | - | 1.5 |
| 50 | 473 | 0.83(0.03) | 0.71 | 0.67 | - |
| 10 | 523 | 17.9 | 19.1 | 18.5 | 19.4 |
| 15 | 523 | 16.0 | 16.6 | 16.3 | 17.0 |
| 23 | 523 | 12.6 | 12.7 | 12.4 | 13.8 |
| 40 | 523 | 5.0 | 5.0 | 4.2 | 5.3 |

* the column headings F(r), RIS and extrap. refer to the use of equation (4) directly, from the RIS model and extrapolation of $D_H$ to $r_{up}$=0.

**Concentration Dependence of $D_H(r)$ at Large H Contents and the Derivation of $D_H^*$ from these Values**

The $Pd_{0.77}Ag_{0.23}$ alloy has been chosen to examine the concentration-dependence of $D_H$ over a wide concentration range. The only method for obtaining $D_H^*$ from $D_H$ appropriate at large $r$ is *via* equation (3) with F($r$) obtained from equilibrium isotherms.

Some results for large $r$ are shown in Figure 16 at 423 K plotted as RT ln $D_H$ against $r_{up}$. There is a minimum in RT ln $D_H$ at $r\approx0.20$. The results of the conversion are shown by the open symbols where two different evaluations of F($r$) were employed with similar results. The $D_H^*$ obtained are not constant but decrease at about $r$=0.07 and then stay approximately constant from $r$=0.16 to 0.27.

Salomons, et al [9, 10] following Wicke and coworkers [5, 18] employ an interstice availability factor in addition to f($r$) where for pure Pd, equation (1) would become

$$D_H(r)=D_H^*(1-r)\left(\frac{\partial \ln p_{H_2}}{\partial \ln r}\right)_T^{1/2}=(1-r)f(r)D_H^* \tag{7}$$

where $(1-r)$ is the interstice availability factor. Instead of equation (3) for the present situation where $r_{up}>>r_{down}$, the expression which includes $(1-r)$ is

$$D_H = D_H^*\left(\frac{F(r)}{r_{up}}\right)-\left(\int_0^{r_{up}} rf(r)dr\right)/r_{up} \tag{8}$$

This equation has been employed for the $Pd_{0.77}Ag_{0.23}$ (Fig. 16) and the the results are shown where the deviations from $D_H^*$ become large especially at high $r$. The $(1-r)$ factor may be too simple for an alloy if blocking of the Pd-rich sites is a factor but it would seem that the correction would be even greater. In any case, even for Pd, it is not certain that this factor is correct because the H atoms undergo extremely rapid jumping and may leave an interstice as one enters it so that $(1-r)$ may be inappropriate.

A minimum is seen in RT ln $D_H$ versus $r$ (Fig. 15) and the conditions can be obtained from (dln $D_H$/d$r$)=0 using equation (3). This leads to the condition that the effective thermodynamic factor from equation (3), $F(r_{up})/r_{up}$ is equal to $f(r_{up})$ . For the present conditions, $r_{up} >> r_{down}$, when the effective thermodynamic factor is equal to $f(r_{up})$ a minimum occurs at $r_{up}$. For the data in Figure 7, $F(r_{up})/r_{up}$ =0.65 at the minimum where $f(r_{up})$=0.67 which is within experimental error. At $r_{up}$ values smaller than the minimum, $F(r_{up})$ / $r_{up}$ > $f(r_{up})$ because the bulk of the membrane has H concentrations less than $r_{up}$) where $f(r)$> $r_{up}$ and at $r_{up}$)> the minimum, $F(r_{up})/r_{up}$<$f(r_{up})$ because $F(r)/r$ will be smaller than $f(r_{up})$.

**Concentration-Independent $E_D^*$ and $\overset{\circ}{D}_H^{*}$ from Concentration-Dependent Values.**

The activation energy for diffusion, $E_D$, is also affected when the thermodynamic factor, $f(r) \neq 1.0$. This has been illustrated for Pd–H where $E_D$ *increases* with $r$ [13]. When equation (3) is differentiated with respect to 1/T, at constant $r_{up}$, equation (7) is obtained. since at constant $r_{up}$, the ln $r_{up}$ term drops out

$$E_D = E_D^* - R\left[\left(\frac{\partial \ln F(r_{up})}{\partial(1/T)}\right) - \left(\frac{\partial \ln r_{up}}{\partial(1/T)}\right)\right] = -R\left(\frac{\partial \ln F(r_{up})}{\partial(1/T)}\right)_{r_{up}}. \tag{9}$$

The activation energy for diffusion has been determined here generally at constant $r_{up}$, e.g., Fig. 6 and therefore the role of non-ideality is given by the change of ln $F(r_{up})$ with 1/T.

Using the RIS model with equation (7), equation (8) can be obtained by differentiating the log terms with respect to 1/T.

$$E_D = E_D^* + \frac{h_1 r_{up}}{[2\ln(1 - r_{up})/r_{up}] - g_1 r_{up}/RT}. \tag{10}$$

Using the dependence of ln $F(r_{up})$ on 1/T, e.g., from figures like 14 at different temperatures, in equation (9) $E_D^*$ proved to be reasonably good at large $r_{up}$ to obtain $E_D^*$ but not at lower values where small differences of ln $F(r_{up})$ become important; this method was therefore not generally employed, however, the $E_D^*$

which was determined large $r$, e.g., at $r$=0.06 and 0.08 for the $Pd_{0.77}Ag_{0.23}$ alloy, appeared to be reasonable.

Since $h_1$ is negative for alloys with $X_{Ag} \leq 0.40$ [7], it would be expected from equation (10) that $E_D(r) > E_D^*$ at least at relatively small values of $r_{up}$. With increase of $X_{Ag}$, $|h_1|$ decreases [7] and $E_D^*$ will approach $E_D$. When $h_1$ becomes positive for, e.g., the $X_{Ag}$=0.50 alloy, then $E_D^* > E_D(r)$ . Figures 9-12 confirm these predictions.

From equation (10) at small $r$, $(\partial E_D/\partial r)_T = -h_1/2$ . Figures 9 and 10 show that the $h_1$ must be more negative than $g_1$ because the slopes with respect to $r$ are greater for $E_D$ than for $RT \ln D_H$. Figure 13 shows that $(\partial E_D/\partial r)_T$ becomes less positive with $X_{Ag}$. From Figures 9, and 10, the values of $h_1$ obtained from the slopes are $-80$ kJ/ mol H and $-75.0$ kJ/ mol H for the $Pd_{0.90}Ag_{0.10}$ and $Pd_{0.77}Ag_{0.23}$ alloys, respectively, where the latter is based on some additional data not shown in Figure 10. It is difficult to compare these to values of $h_1$ from thermodynamics which are not very accurate for these Pd–Ag alloys. The approximations for the slopes are only good at small $r$ and thereafter the complete equations, e.g., equation (10), must be employed which are themselves, approximations.

The concentration-independent Arrhenius equation for interstitial diffusion is

$$D_H^* = D_H^{\circ,*} \exp^{-E_D^*/RT}$$  (11)

$D_H^{\circ,*}$ values given in Table 6 have been calculated from $D_H^*$ and $E_D^{\circ,*}$ . The values of $D_H^{\circ,*}$ are between 3.4 and $4.9 \times 10^{-3}$ cm$^2$/s with no clear trend with $X_{Ag}$. Holleck [3] and Wicke and Brodowsky [8] found small decreases with $X_{Ag}$ but the latter indicate that there is not much change with $X_{Ag}$ for deuterium which seems to be inconsistent with their results for H. $E_D^*$ appears to be smaller for the $Pd_{0.90}Ag_{0.10}$ alloy than for Pd as was found in reference [8]. It is possible that the lattice expansion due to Ag lowers $E_D^*$ while other factors which enter at greater $X_{Ag}$ are not very important for the $Pd_{0.90}Ag_{0.10}$ alloy.

Table 6:  Concentration Independent $E_D^*$/kJ/ mol H and $D_H^{\circ,*}$ Values (423-523 K)

| % Ag | $D_H^*(473K)/cm^2/s$ | $E_D^*$ | $D_H^{*\circ}/cm^2/s$ |
|---|---|---|---|
| 0 | $13.3\times10^{-6}$ | 23.9 | $5.6\times10^{-3}$ |
| 10 | $10.7\times10^{-6}$ | 23.7 | $3.4\times10^{-3}$ |
| 15 | $9.7\times10^{-6}$ | 23.9 | $4.2\times10^{-3}$ |
| 19 | $9.1\times10^{-6}$ | 24.3 | $4.0\times10^{-3}$ |
| 23 | $8.0\times10^{-6}$ | 24.1 | $3.7\times10^{-3}$ |
| 30 | $5.9^{10-6}$ | 26.1 | $4.5\times10^{-3}$ |
| 35 | $4.2\times10^{-6}$ | 27.7 | $4.8\times10^{-3}$ |
| 40 | $2.7\times10^{-6}$ | 29.4 | $4.8\times10^{-3}$ |
| 45 | $1.5\times10^{-6}$ | 30.6 | $3.6\times10^{-3}$ |
| 50 | $0.69\times10^{-6}$ | 34.9 | $4.9\times10^{-3}$ |

The permeability of the $Pd_{0.77}Ag_{0.23}$ alloy is greater than that of the others at 50.6 kPa and e.g., 423 K, (Fig. 4) despite the fact that at this $p_{H_2}$, $r$ is greater for alloys with $X_{Ag}$<0.23. An example is the $Pd_{0.85}Ag_{0.15}$ alloy whose solubility at 50.6 kPa (423 K) is $r$=0.36 as compared to 0.28 for the $Pd_{0.77}Ag_{0.23}$ alloy and at this temperature $D_H^*$=4.7×10$^{-6}$/cm$^2$/s for the former and 4.0×10$^{-6}$/cm$^2$/s for the latter. The answer to this apparent contradiction is that f($r$) is smaller, i.e., at 50.6 kPa (423 K), f($r$)=0.54 for the $Pd_{0.85}Ag_{0.15}$ alloy and f($r$)=0.88 for the $Pd_{0.77}Ag_{0.23}$ alloy. The permeability is given by $P$=f($r$)$D_H^*c_{up}$ and, from the above values, the ratio $P(Pd_{0.77}Ag_{0.23})/P(Pd_{0.85}Ag_{0.15})$=1.08. According to Figure 4 the ratio is 1.3 which is greater than this predicted value but it is in the right direction to explain the greater $P$ of the $Pd_{0.77}Ag_{0.23}$ alloy.

# Concentration Profiles for the $Pd_{0.77}Ag_{0.23}$ Alloy Membrane when $p_{up} >> p_{down}$

Concentration profiles can be determined using equation (12) [12]

$$F(r)=F(r_{up})\left(1-\frac{x}{d}\right)$$

(12)

where x is the distance through the membrane and x=0 and d correspond to the upstream and downstream sides, respectively. In order to determine the profile for a given $r_{up}$, values of F(r) can be calculated as a function of $r$; with these F(r) and F($r_{up}$) , (x/d) can be calculated from equation (12). The F(r) versus $r$ plot for the $Pd_{0.77}Ag_{0.23}$ alloy is shown in Figure 16. For a given alloy and temperature, the F(r)–r relation has a unique shape. Also shown in the Figure is the relation calculated from the RIS model using equation (6) with $g_1$=–22.7 kJ/ mol H. The agreement is quite good but only up to about $r$=0.12.


Values of (x/d) have been calculated to determine the concentration profiles shown in Figure 18 for the $Pd_{0.77}Ag_{0.23}$ alloy at 20.3 kPa and at 50.6 kPa (423 K). It is seen that, except for the limiting values of (x/d)=0 and 1.0, the H concentrations are larger at 50.6 kPa than the ideal ones but at 20.3 kPa, the concentrations are smaller. From Figure 14 at 20.3 kPa, $r$=0.15 and at this $r_{up}$, F($r_{up}$)=0.10 (Fig. 17). For 50.6 kPa, $r_{up}$=0.28 (Fig. 14) and from Figure 17, F($r_{up}$)=0.235.


It is of interest that the deviations of $r$ from ideality are positive for 50.6 kPa ($r_{up}$=0.28) and negative for 20.3 kPa ($r_{up}$=0.15) (Fig. 18). For the former at $r_{up}$=0.28, f(r) is >1.0 and for the latter at $r_{up}$=0.15, f(r)<1.0 (Fig. 15). From $J=-D_H(c_H)\left(\partial c_H/\partial x\right)= -D_H^*f(r)\left(\partial c_H/\partial x\right)$ , it follows that at $r_{up}$=0.28, $\left(\partial c_H/\partial x\right)$ will be less negative than the ideal slope, $c_{up}/d$, and for $r_{up}$=0.15 (Figs. 15, 18) with f($r_{up}$)>1.0, $\left(\partial c_H/\partial x\right)$ must be more negative than the ideal slope. If f($r_{up}$) is >1.0, the deviations will be positive and if f($r_{up}$) is <1.0, the deviations will be negative.

In the steady state, the flux is constant throughout a membrane, i.e., $J=-D_H(c_H)\left(\partial c_H/\partial x\right)$ where $D_H(c_H)$ and $\left(\partial c_H/\partial x\right)$ change with x but in the steady state, they compensate each other to maintain J constant at all x and corresponding $r$. J must also be equal to the measured steady state value, $-D_H\left(c_{H,up}/d\right)$ and it must also be equal to $-D_H^*\left(c_H/RT\right)\left(\partial m_H(r)/\partial x\right)$. Calculated values of these various fluxes from these equations are closely equal for the $Pd_{0.77}Ag_{0.23}$ alloy.

## Conclusions

It is shown from the linearity of plots of J against 1/d that bulk diffusion is the slow step for the Pd–Ag alloy with the greatest permeability, $Pd_{0.77}Ag_{0.23}$. The permeabilities of the alloys at $p_{up}$=20.3 and 50.6 kPa are a maximum at about $X_{Ag}$ =0.23 for the temperature range: 423-523 K. The permeability in the $Pd_{0.77}Ag_{0.23}$ alloy is shown to be nearly independent of temperature at $p_{H_2}$=20.3 kPa because $c_H$ and $D_H$ compensate each other, i.e., $c_H$ decreases with temperature increase while $D_H$ increases.

The dependence of $D_H$ on $X_{Ag}$ has been determined at a given $p_{up}$ and $D_H$ is nearly constant up to $X_{Ag}\approx0.30$ and then, $D_H$ values fall-off more sharply.

It was shown elsewhere [13] that $D_H$ and $E_D$ vary significantly with $r$ in the dilute phase of Pd–H. The dependence of these parameters have been examined here for the Pd–Ag alloys and the dependence of $D_H$ and $E_D$ on $r$ depends on $X_{Ag}$. $D_H$ decreases with H concentration for the alloys up to $X_{Ag}\approx0.35$ where there is only a negligible effect. $E_D$ increases with H concentration for alloys with $X_{Ag}$<0.35. These results are related to the thermodynamic factor and its change with $X_{Ag}$.

It is often assumed that Einstein's concentration-independent diffusion constant cannot be obtained by permeation measurements with large concentration gradients, e.g., [11], however, it is shown here that this is not the case and $D_H^*$ and $E_D^*$ values have been obtained for these alloys. The dependence of $D_H$ on $r$ has been examined over a large range of H contents for the $Pd_{0.77}Ag_{0.23}$ alloy and these have been converted to concentration-independent $D_H^*$, however, they are not constant for $r$ >0.15 but increase slightly.

# References

1.  M. Chowdbury, D. Ross, *Solid State Comm.,* **13** (1973) 229.

2.  O. Lovvik, R. Olson, *J. Alloys Compounds,* **330-332** (2002) 332.

3.  G. Holleck, *J. Phys. Chem.,* **74** (1970) 503.

4.  A. Küssner, *Z. Naturforschung*, 21a (1966) 515.

5.  G. Bohmholdt, E. Wicke, *Zeit. Physik. Chem. N.F.*, **56** (1967) 133.

6.  L. Opara, B. Klein, H. Züchner, *J. Alloys Compounds,* **253-254** (1997) 378.

7.  T. Flanagan, D. Wang, S. Luo, *submitted for publication.*

8.  E. Wicke, H. Brodowsky, in *Hydrogen in Metasl, II* G. Alefeld, J. Völkl, eds., Springer-Verlag, Berlin, 1978.

9.  E. Salomons, PhD thesis, Vrije Univ., Amsterdam, 1989.

10. E. Salomons, U. Ljungblad, R. Griessen, *Defect and Diffusion Forum*, **66-69** (1989) 327.

11. P. Stonadge, M. Benham, D. Ross, C. Manwaring, I. Harris, *Z. Physik. Chem.,* **181** (1993) 125.

12. T. Flanagan, D. Wang, K. Shanahan, *Scripta Mater.,* **56** (2007) 261.

13. T. Flanagan, D. Wang, K. Shanahan, *to be published*.

14. D. Wang, T. Flanagan, K. Shanahan, *J. Membrane Sci.,* **253** (2005) 165.

15. E. Serra, M. Kemali, A. Perujo, D. Ross, *Met. Mater. Trans. A* **29A** (1998).

16. R. Lässer, L. Powell, *J. Alloys Compounds,* **130** (1987) 387.

17. W. Oates, T. Flanagan, *J. Materials Sci.*, **16** (1981) 3235.

18. G. Holleck, E. Wicke, *Z. Physik. Chem. N.F.,* **56** (1967) 155.

**Figure Captions**

**Fig. 1.** $H_2$ permeability plotted against $p^{1/2}$ at 473 K for the $Pd_{0.77}Ag_{0.23}$ alloy membrane. ○, experimental data; Δ, data corrected for deviations from Sieverts' law of ideal solubility.

**Fig. 2.** $H_2$ flux plotted against 1/d for $Pd_{0.77}Ag_{0.23}$ alloy membranes at 473 K and 50.6 kPa.

**Fig. 3.** $H_2$ permeabilities plotted against atom % Ag for $p_{up}$=20.3 kPa at 423, 473 and 523 K.

**Fig. 4.** $H_2$ permeabilities plotted against atom % Ag for $p_{up}$=50.6 kPa at 423, 473 and 523 K.

**Fig. 5.** Log $D_H$ determined at $p_{H_2}$=20.3 kPa for the present data plotted against $X_{Ag}$ at 473 K. ○, present data; Δ, ref. [3]; □, ref. [15].

**Fig. 6.** Quantity $\alpha \ln J$ plotted against 1/T for Pd–Ag membranes at different, but constant, $r_{up}$. The $X_{Ag}$ of the alloys is indicated.

**Fig. 7.** $E_D$ and $E_P$ plotted against $X_{Ag}$ determined from the data in Figure 6.

**Fig. 8.** Diffusion data for the $Pd_{0.77}Ag_{0.23}$ alloy determined at $p_{up}$=20.3 kPa. ○, log $D_H$/cm$^2$/s, Δ, log$c_H$/mol H/cm$^3$ and □, sum of the plots for log $D_H$ and log$c_H$ translated along the y-axis in order to correspond to the intersection of the log $D_H$ and log$c_H$ plots.

**Fig. 9.** RT ln $D_H$ and $E_D$ as a function of $r$ at 423 K for the $Pd_{0.90}Ag_{0.10}$ alloy.

**Fig. 10.** RT ln $D_H$ and $E_D$ as a function of $r$ at 473 K for the $Pd_{0.77}Ag_{0.23}$ alloy.

**Fig. 11.** RT ln $D_H$ and $E_D$ as a function of $r$ at 473 K for the $Pd_{0.65}Ag_{0.35}$ alloy.

**Fig. 12.** RT ln $D_H$ and $E_D$ as a function of $r$ at 473 K for the $Pd_{0.50}Ag_{0.50}$ alloy.

**Fig. 13.** Plots of RT ln $D_H$ against $r$ at 423 K for the four alloys shown.

**Fig. 14.** Isotherms for the $Pd_{0.77}Ag_{0.23}$ alloy plotted as $\ln p^{1/2}$ as a function of $\ln r$.

**Fig. 15.** Thermodynamic factor plotted against $r$ at 423 K for the $Pd_{0.77}Ag_{0.23}$ alloy. The vertical dashed line indicates ideal behavior where $f(r)=1.0$.

**Fig. 16.** RT $\ln D_H$ against $r$ over a large H content (423 K). ●, experimental data; ○, △ , values using equation (3) from two different sets of F(r)-r relations; ▲, using equation (3) with the (1-r) factor included.

**Fig. 17.** F(r) against $r$ for the $Pd_{0.77}Ag_{0.23}$ alloy at 423 K. ○, experimental F(r); △, F(r) from RIS model.

**Fig. 18.** H-to-metal ratio in the membrane, $r$, plotted against distance, (x/d), through the membrane for the $Pd_{0.77}Ag_{0.23}$ alloy at 423 K. ○, at 50.6 kPa; △, 20.3 kPa. The full straight lines indicate ideal behavior where $f(r)=1.0$.

**Figure 1.**



**Figure 2.**

**Figure 3.**



P$_{H2}$ = 20.26 kPa

○, 523 K
□, 473 K
△, 423 K

Perm *$10^8$/(mol H cm/s cm$^2$)

Ag at%

**Figure 4.**



P$_{H2}$ = 50.6 kPa

Perm* $10^8$ /(mol H cm/s cm$^2$)

523 K
473 K
423 K

Ag at%
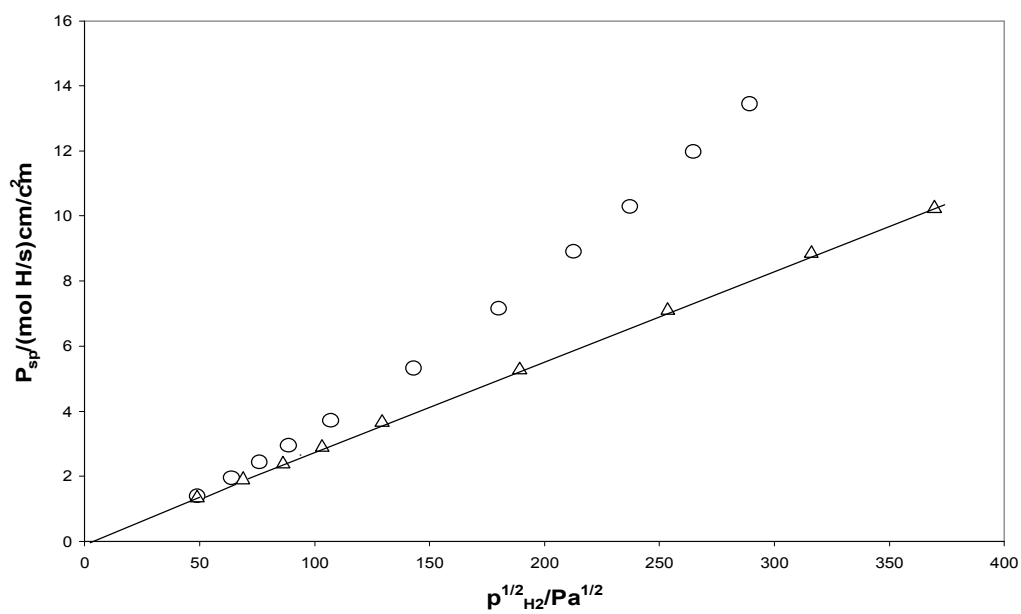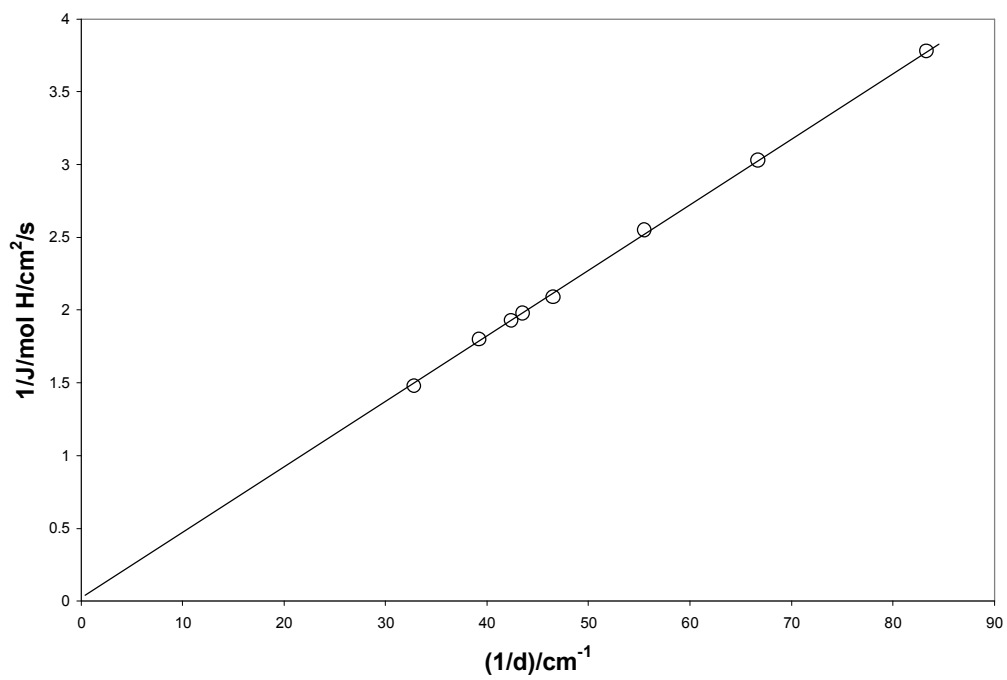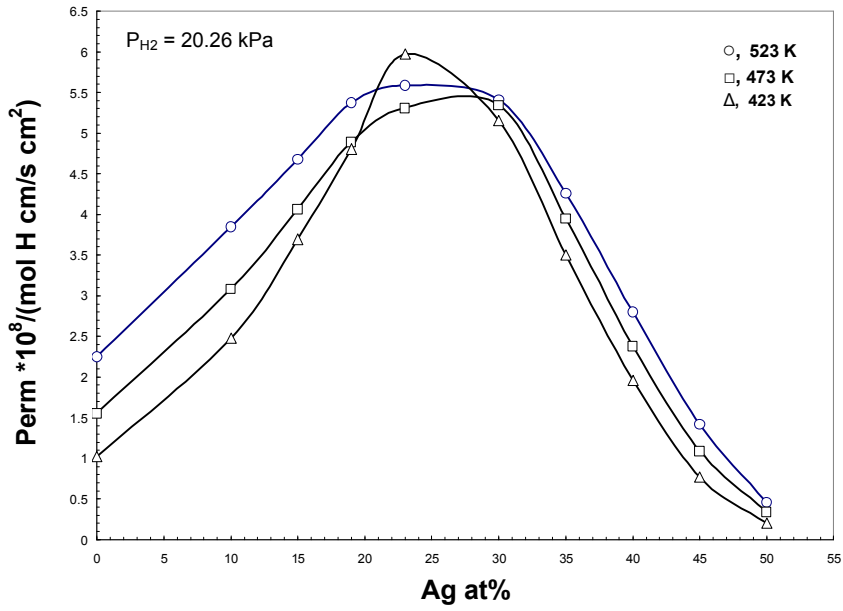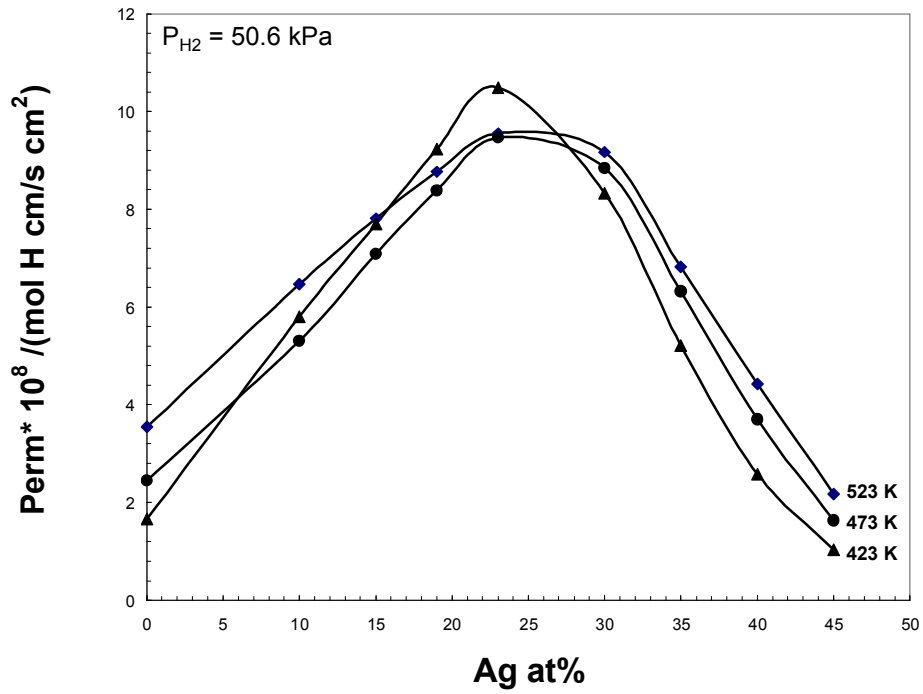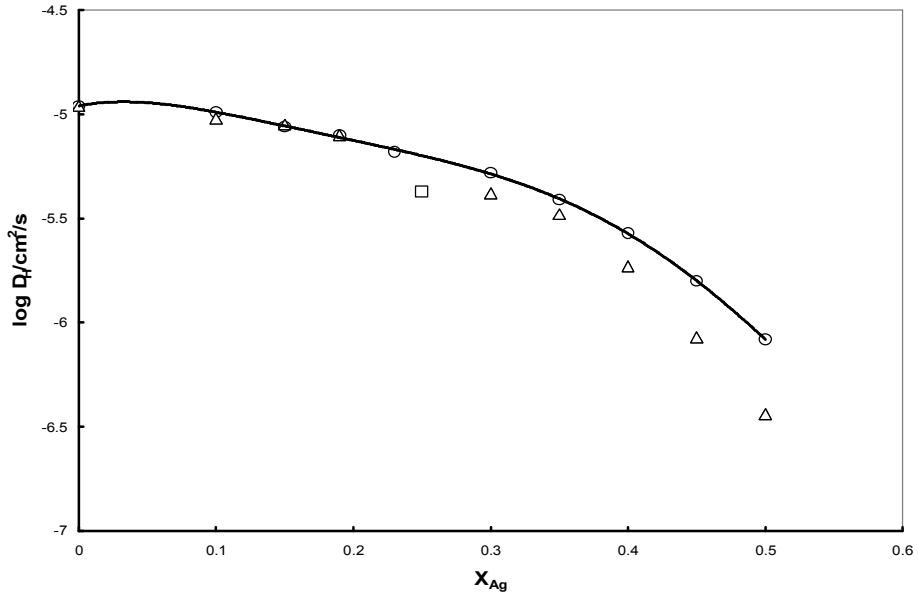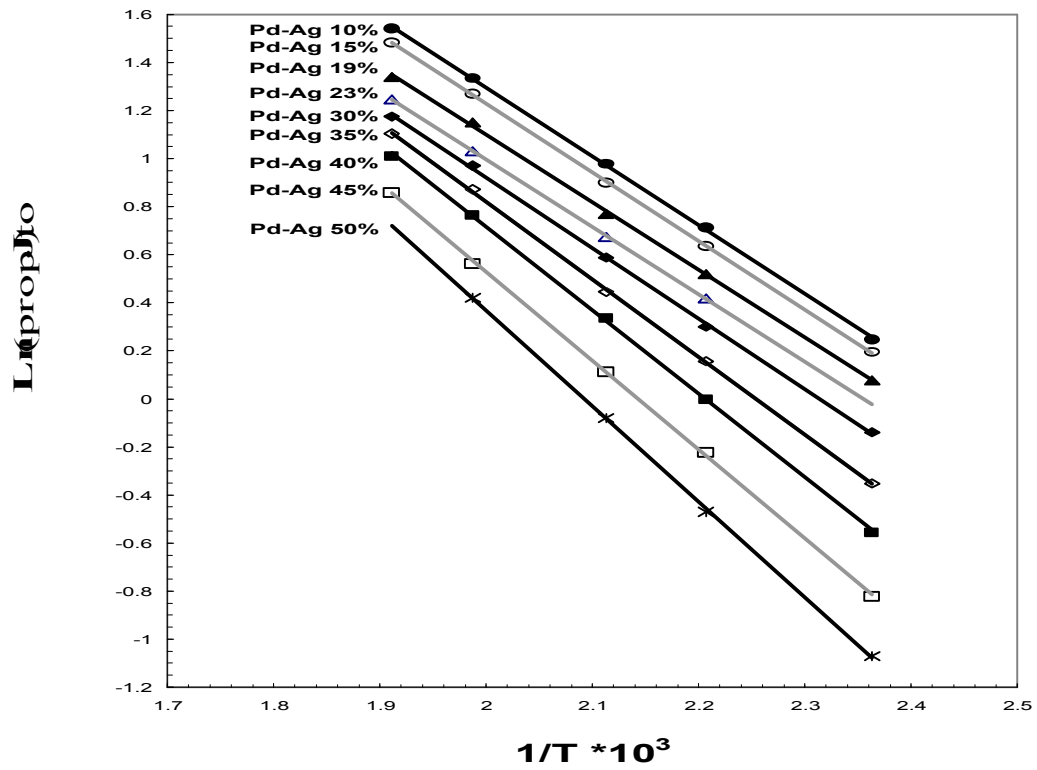
**Figure 5.**



**Figure 6.**

**Figure 7.**
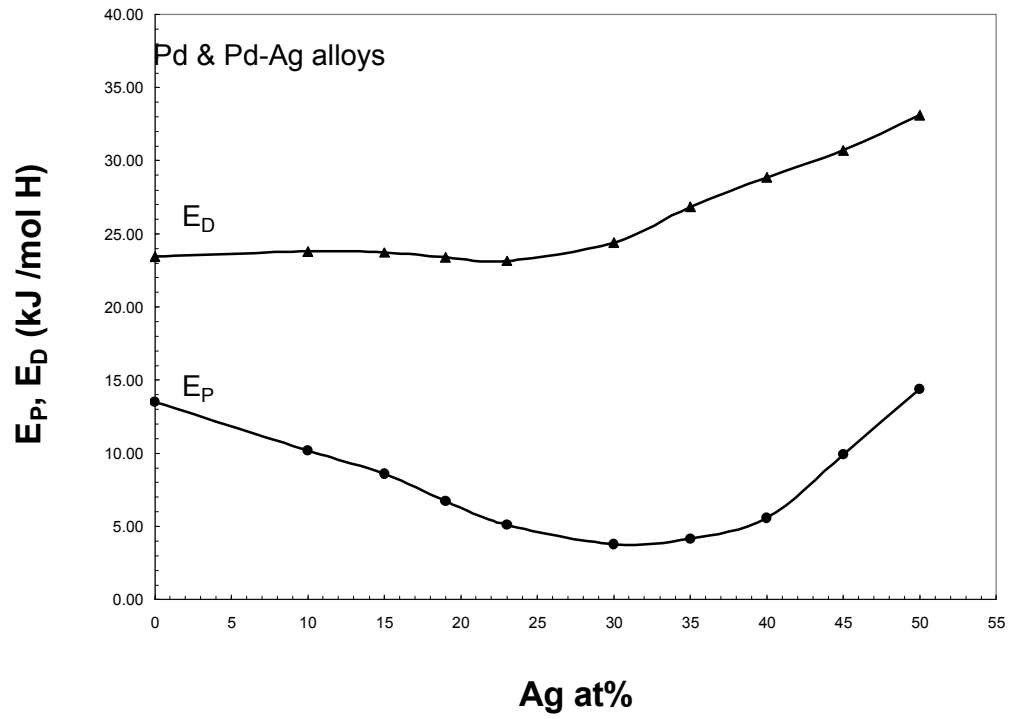


**Figure 8.**
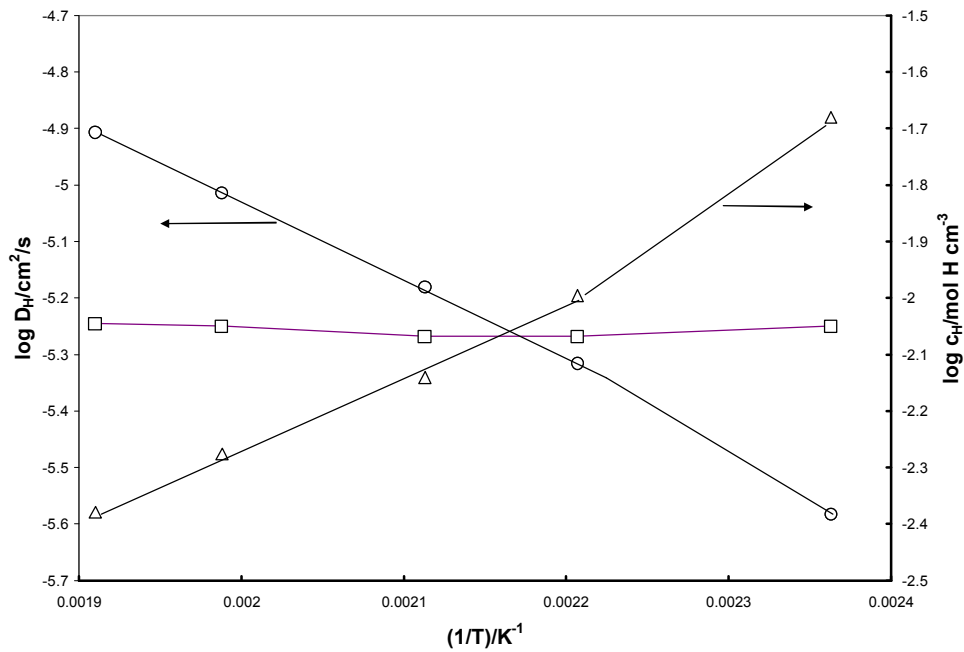
**Figure 9.**
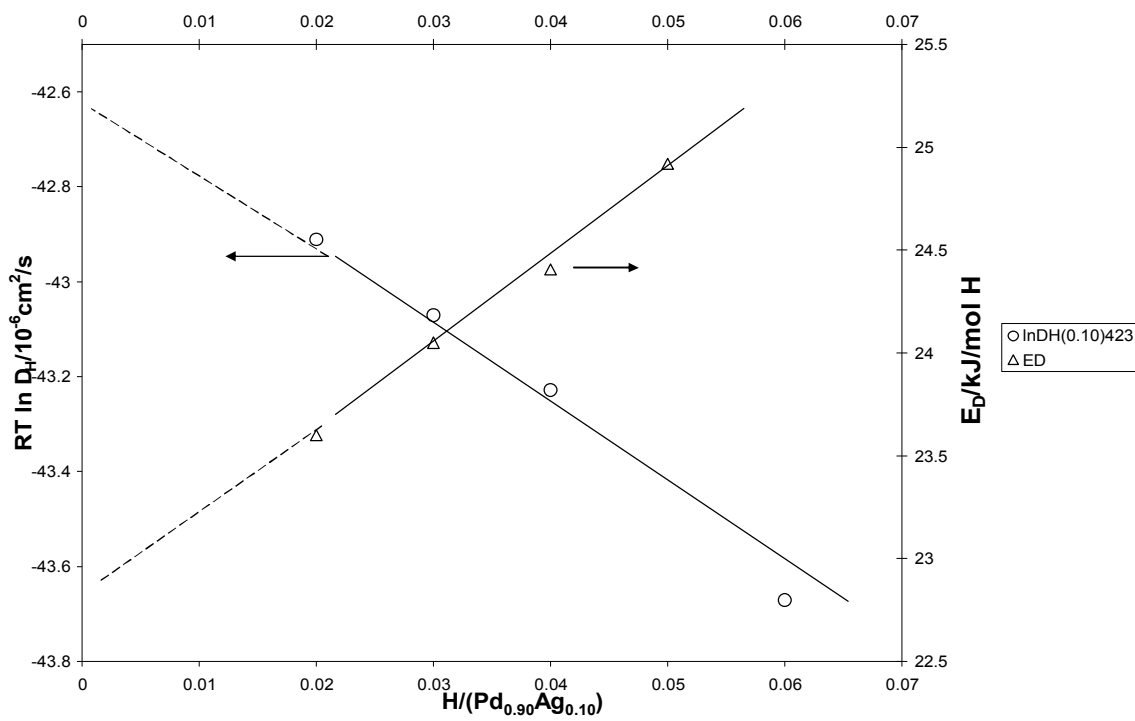


**Figure 10.**
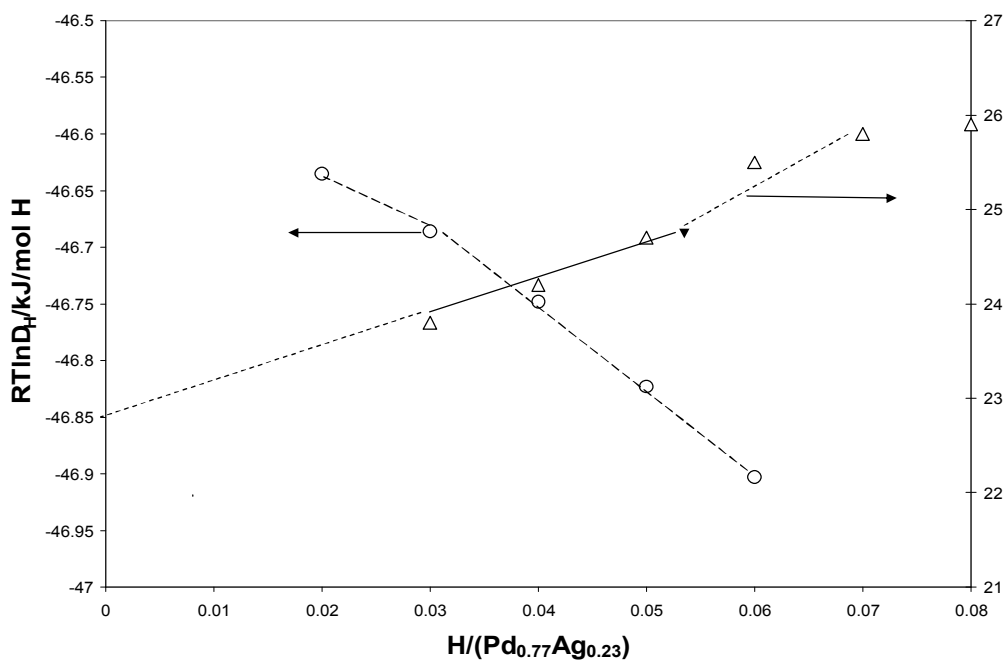
**Figure 11**
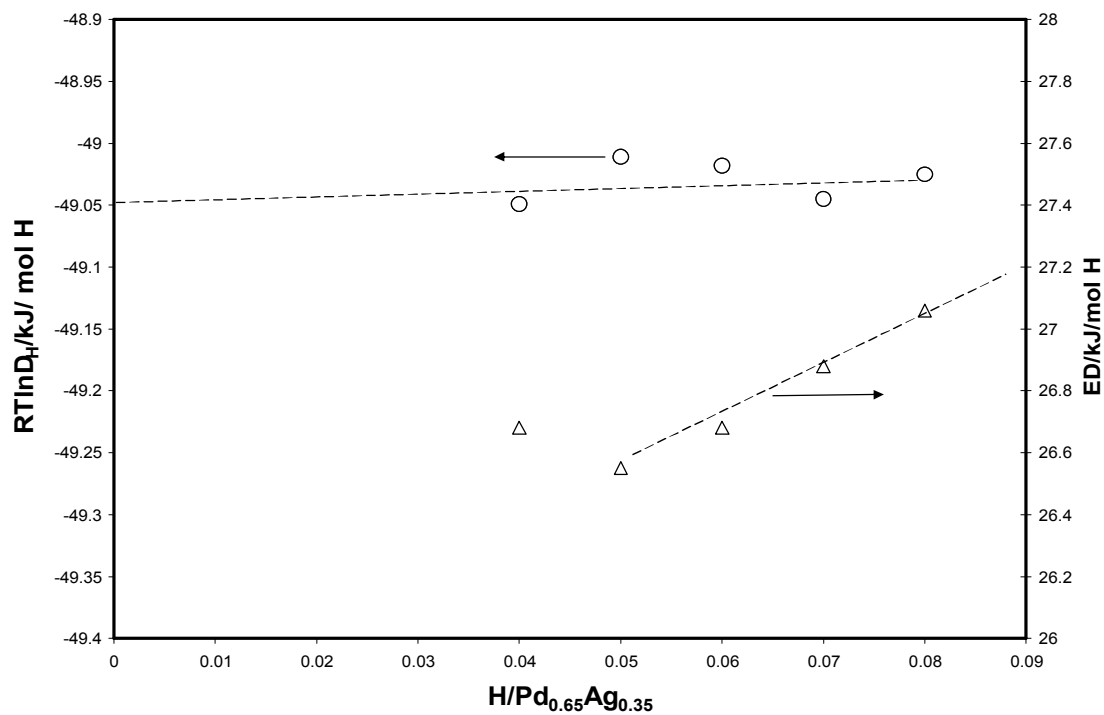


**Figure 12.**
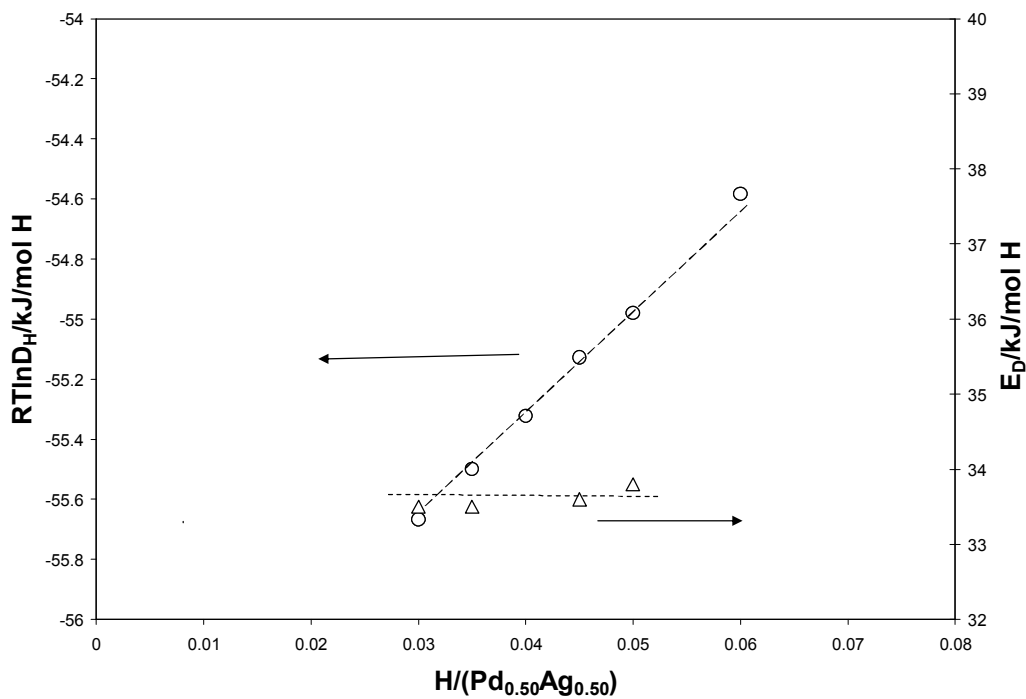
**Figure 13.**
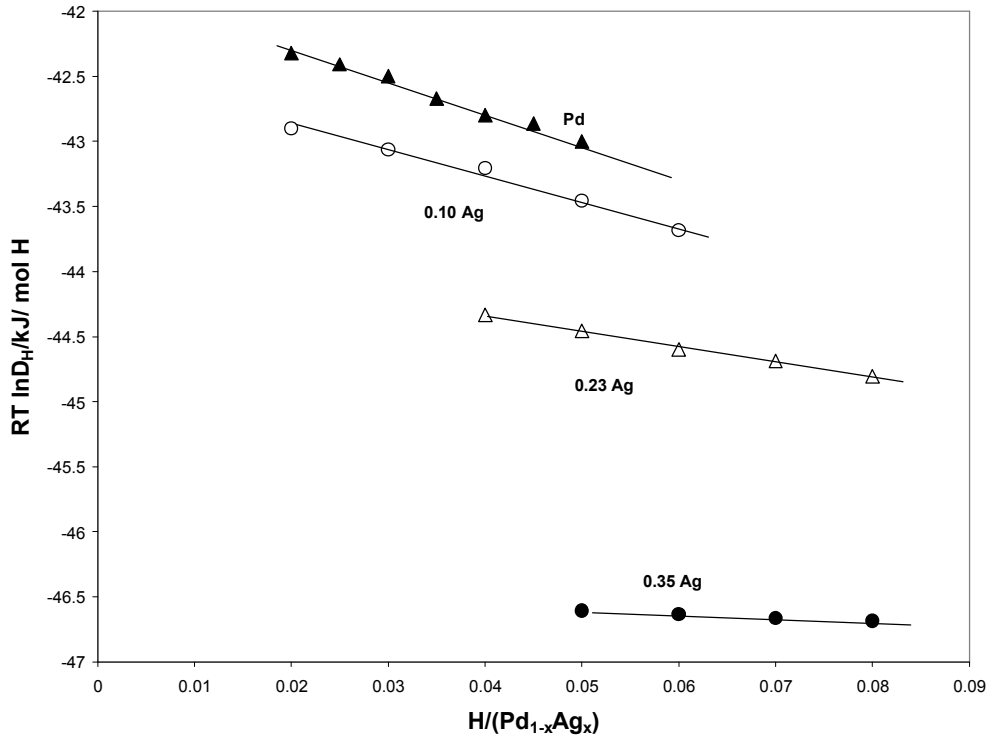


**Figure 14.**
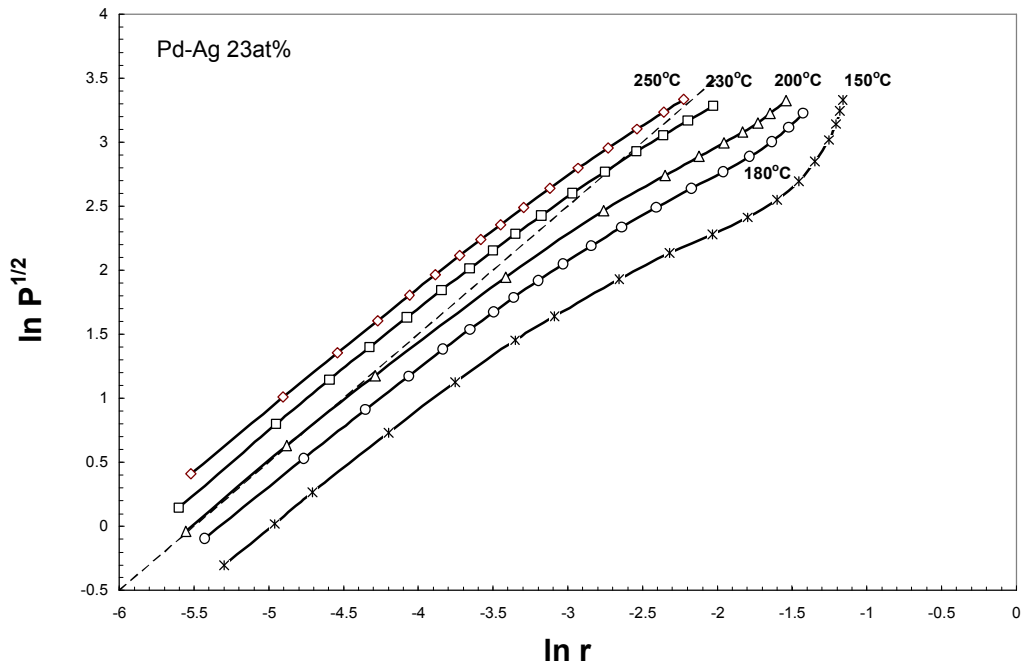
**Figure 15.**
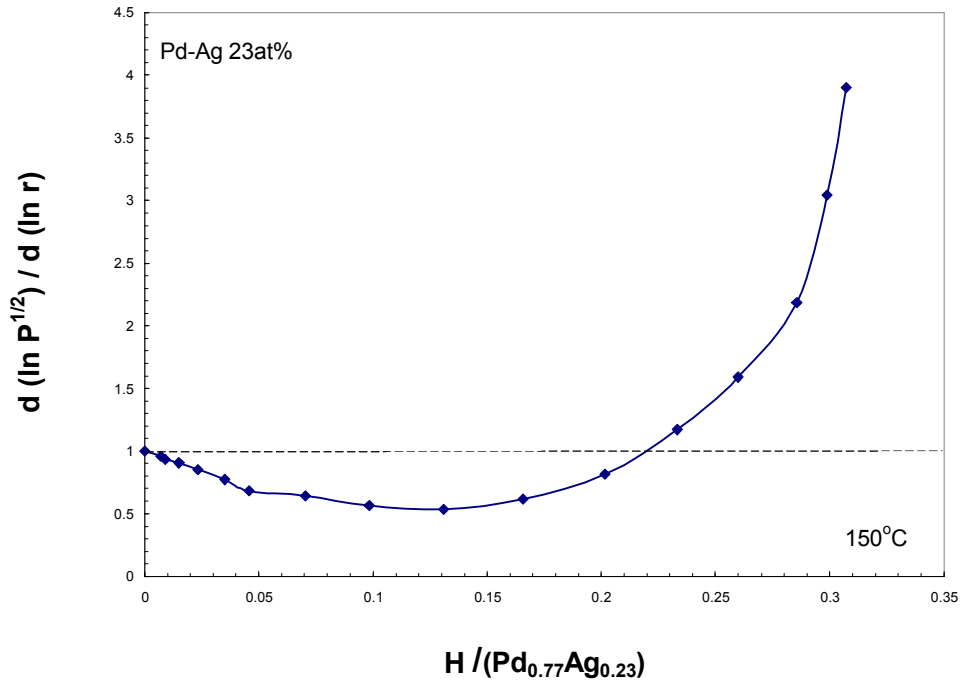


**Figure 16.**

**Figure 17.**



**Figure 18.**